

Time-resolved demagnetization of Co_2MnSi observed using x-ray magnetic circular dichroism and an ultrafast streak camera

This article has been downloaded from IOPscience. Please scroll down to see the full text article.

2010 J. Phys.: Condens. Matter 22 156003

(<http://iopscience.iop.org/0953-8984/22/15/156003>)

View [the table of contents for this issue](#), or go to the [journal homepage](#) for more

Download details:

IP Address: 129.252.86.83

The article was downloaded on 30/05/2010 at 07:47

Please note that [terms and conditions apply](#).

Time-resolved demagnetization of Co₂MnSi observed using x-ray magnetic circular dichroism and an ultrafast streak camera

Y P Opachich^{1,2}, A Comin³, A F Bartelt⁴, A T Young¹, A Scholl¹,
J Feng¹, J Schmalhorst⁵, H J Shin⁶, K Engelhorn¹, S H Risbud²,
G Reiss³ and H A Padmore¹

¹ Lawrence Berkeley National Laboratory, Berkeley, CA 94720-8099, USA

² Department of Chemical Engineering and Materials Science, University of California at Davis, Davis, CA 95616, USA

³ Italian Institute of Technology, Nanophys, 16163 Genova GE, Italy

⁴ Department of Materials for Photovoltaics, Helmholtz Center Berlin for Materials and Energy, 14109 Berlin, Germany

⁵ Department of Physics, Bielefeld University, 33501 Bielefeld, Germany

⁶ Pohang Accelerator Laboratory, Pohang University of Science and Technology, Kyungbuk 790-784, Korea

E-mail: YPOpachich@gmail.com

Received 2 February 2010

Published 29 March 2010

Online at stacks.iop.org/JPhysCM/22/156003

Abstract

The demagnetization dynamics of the Heusler alloy Co₂MnSi was studied using picosecond time-resolved x-ray magnetic circular dichroism. The sample was excited using femtosecond laser pulses. In contrast to the sub-picosecond demagnetization of the metal ferromagnet Ni, substantially slower demagnetization with a time constant of 3.5 ± 0.5 ps was measured. This could be explained by a spin-dependent band gap inhibiting the spin-flip scattering of hot electrons in Co₂MnSi, which is predicted to be half-metallic. A universal demagnetization time constant was measured across a range of pump power levels.

(Some figures in this article are in colour only in the electronic version)

1. Introduction

Ultrafast optical control of magnetization is one of the challenges of contemporary magnetism. Although ultrafast laser-induced demagnetization has been shown to occur within several hundreds of femtoseconds in ferromagnetic metals [1–6], the demagnetization route is still a subject of debate. Spin-flip scattering of hot electrons is the most commonly accepted demagnetization mechanism, occurring at a several orders of magnitude faster timescale (~ 100 fs) [1, 5–8] than switching caused by the application of an external magnetic field. Upon laser excitation, nascent electrons thermalize through electron–electron and electron–phonon scattering [9]. The Elliot–Yafet process

has been discussed as the mechanism facilitating ultrafast demagnetization in ferromagnetic metals [7]. In electron transport, this mechanism is the source of spin relaxation and depolarization at magnetic impurities. Spin–orbit coupling couples spin-up and spin-down electronic states that are close in energy and angular momentum is transferred to phonons.

A prerequisite for spin-flip scattering is the availability of empty minority states at the Fermi level. For this reason, a reduction in or lack of available minority phase space should therefore limit spin-flip events and slow down the demagnetization after an ultrafast excitation. Half-metals are a perfect system to test this hypothesis [10]. The majority states of a half-metal have metallic character, while the minority states exhibit a band gap. This band gap can lead to a close

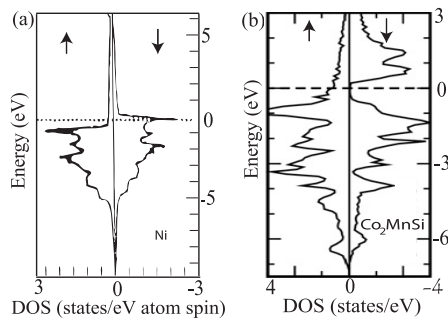


Figure 1. (a) and (b) Schematic of Ni and Co_2MnSi electronic DOS for the majority and minority of spins labeled down and up respectively [15, 16].

to 100% spin polarization of the Fermi level and makes half-metals useful for spintronics applications. Demagnetization times in the 100 ps range have been observed using optical spectroscopy in several systems that are believed to be half-metals [11–13]. In a comparative study of materials believed to be half-metallic Müller *et al* observed a general increase of the demagnetization time with increasing spin polarization at the Fermi level [10]. In the same study, Co_2MnSi exhibited sub-ps demagnetization comparable to that of Ni although band structure calculations of the Heusler alloy, Co_2MnSi , predict a half-metallic minority state band gap of ~ 1 eV, as shown in figure 1(b). The majority electron occupied Co_2MnSi 3d band consists of Mn electrons, while the minority unoccupied states are largely composed of Co e_u and Mn t_{2g} bands [14, 15]. In contrast, Ni, shown in figure 1(a) possesses empty minority 3d states at the Fermi level [16]. The availability of low lying empty states in Ni allows laser excited majority electrons to scatter into unoccupied minority states through spin-flip (Stoner) excitations coupled with a phonon, according to the Elliot–Yafet model, leading to the observed fast demagnetization [6–8]. Tunnel magneto-resistance measurements of $\text{Co}_2\text{MnSi}/\text{Al}-\text{O}/\text{Co}-\text{Fe}$ tunnel junctions showed an enhanced magneto-resistance, indicating an increased effective tunneling spin polarization compared to conventional transition metal alloys [17, 18]. Whether this enhanced spin polarization can lead to a slow down of the demagnetization in the limit of a large degree of demagnetization (close to 100%) is the topic of this paper. The novel technique of picosecond time-resolved x-ray magnetic circular dichroism was used to record the magnetic response of the system after an ultrafast IR laser excitation⁷.

2. Methods

2.1. Sample preparation

The Ni sample was sputter deposited at room temperature (RT) and consisted of a Si_3N_4 membrane, a 100 nm Al heat sink, a 20 nm Ni thin film and a thin (2 nm) Al cap to prevent oxidation. The half-metallic alloy sample was dc-magnetron

⁷ In this work, different substrates, buffer layers, layer thicknesses and a composition optimized target were used in contrast to Müller *et al* [10], Kämmerer *et al* [17] and Schmalhorst *et al* [18].

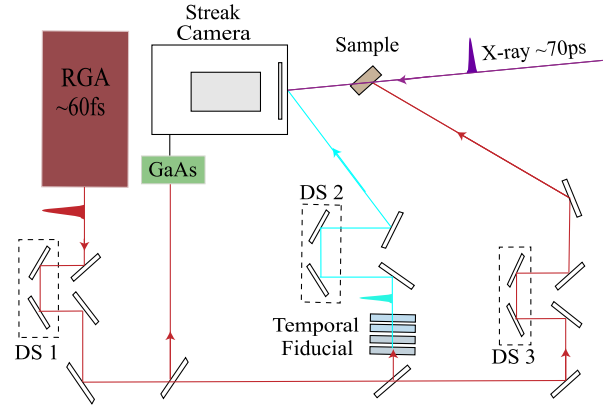


Figure 2. Schematic diagram of the pump–probe experimental setup. The IR beam is divided into three branches: the first beam (~ 500 mW) is used to trigger the streak camera via the GaAs switch, the second beam (~ 700 mW) is passed through a frequency tripling system to produce UV fiducialization and the third is used to heat the sample (~ 100 – 300 mW). The x-ray pulses are produced by a synchrotron and synchronized to the laser system with delay stages 1 and 3. Delay stage 2 is used to synchronize the arrival of the UV pulses at the camera.

sputtered at RT onto an Si_3N_4 window and consisted of a 80 nm Cu heat sink, followed by Ta and V seed layers, 20 nm of Co_2MnSi and 2 nm of Al that was oxidized for 100 s. The thickness of the Co_2MnSi was chosen to match the penetration depth of the IR pump beam. A composition optimized sputter target was used to guarantee that the film composition is very close to the desired value of 2:1:1. The entire sample was then heated to 437°C to improve the sample texture and magnetic properties. The annealing temperature and time were carefully chosen to reach an optimum magnetic moment. At room temperature the Heusler sample exhibited magnetization that is 70% of theoretical predictions for a perfect crystalline sample, with typical values of $\sim 5 \mu_B/\text{f.u.}$ at 0 K [15]. The spin magnetic moment is distributed among the Co and Mn sites with a ratio of ~ 2 – $3 \mu_B/\text{f.u.}$ respectively [15]. In addition to the expected reduction in moment at elevated temperature this indicates an imperfectly ordered Heusler system. The reduced order likely causes a reduction of the spin polarization at the Fermi level due to additional low lying empty minority states. Note that scattering into those states is expected to increase the demagnetization speed and values measured here are a lower limit for those of a perfect half-metallic system. An increase in the demagnetization time constant compared to a simple metal like Ni can thus be interpreted as an indicator for an enhanced spin polarization and possibly the half-metallicity of the Co_2MnSi layer.

2.2. Experimental details

The experimental setup is shown in figure 2. A 5 kHz Ti:sapphire laser system was used to heat the samples, trigger the ultrafast streak camera and to create UV time calibration markers. Both Ni and Co_2MnSi were excited with 60 fs pulses at wavelengths centered near 800 nm and powers of up to $50 \mu\text{J}/\text{pulse}$. The samples were placed in a 20 mT

magnetic field, with the field direction alternated between acquisitions. The magnetic phase transition was probed with 70 ps (FWHM) elliptically polarized x-ray pulses generated by a type-II apple undulator [19, 20] at beam-line 11.0.1 at the Advanced Light Source (ALS). The undulator was tuned to the Ni and Mn L_3 edges in order to probe the element specific number of available minority and majority empty states by the excitation of electrons from the spin-orbit split $p_{3/2}$ -states [21, 22]. The Mn edge was chosen to monitor the Co_2MnSi demagnetization due to a slightly higher magnetic moment, similar demagnetization profiles were observed at the Co edge. Demagnetization data was collected in transmission thus probing the bulk of the sample. The laser was synchronized with the ALS ring frequency by tuning the oscillator frequency and by varying the laser path length with several delay stages, shown in dashed lines in figure 2. The demagnetization information was obtained by temporally dispersing the x-ray pulses in an x-ray streak camera [23–25]. Two UV fiducials of known time separation near the x-ray signal were used for time calibration and for continual monitoring of the detector performance. The x-ray probe diameter was $\sim 100 \mu\text{m}$, while the laser was focused to $\sim 500 \mu\text{m}$ (FWHM), in order to insure that the sampled area was evenly heated. Ni and Co_2MnSi demagnetization signals were collected with either a gated micro-channel plate coupled with a phosphor and a visible light CCD camera or a direct CCD imaging system. When compared, the results obtained from both measurement systems were in agreement.

3. Results

Streak images collected at the Mn L_3 edge are shown in figures 3(a)–(c). The top image (a) was recorded with magnetization orientation, M_s , parallel to the x-ray polarization, σ , while the streak image shown in (b) was collected after changing the orientation of the magnetization M_s to be anti-parallel to the x-ray polarization. Typically, two averaged sets of data were collected at opposite helicity in order to improve statistics. In the experiment, the difference of images (a) and (b), i.e. the dichroic signal, was used to observe changes in the magnetic state of our samples, see figure 3(c). The loss of dichroic signal in figure 3(c) corresponds to the presence of a magnetic phase transition. The time necessary to complete the phase transition, i.e. the demagnetization constant, τ , were determined by fitting the asymmetry data that was extracted from the integrated cross sections of the streak images. The resulting normalized Ni and Co_2MnSi asymmetry plots along with their fits are shown in figure 3(d). It has been previously shown that Ni demagnetizes within ~ 300 fs [1, 4–6, 26], which appears as an instantaneous loss of magnetization at our experimental timescales. For this reason, Ni asymmetry data shown in figure 3(d) was used to determine the detector time resolution by fitting the cross section plot with a convolution of a step function with a Gaussian representing the detector resolution, i.e. an error function. The Ni sample was also used to establish *time zero*, t_0 , which in our experiment appears at the half-point in the demagnetization curve. Care was taken to collect Ni

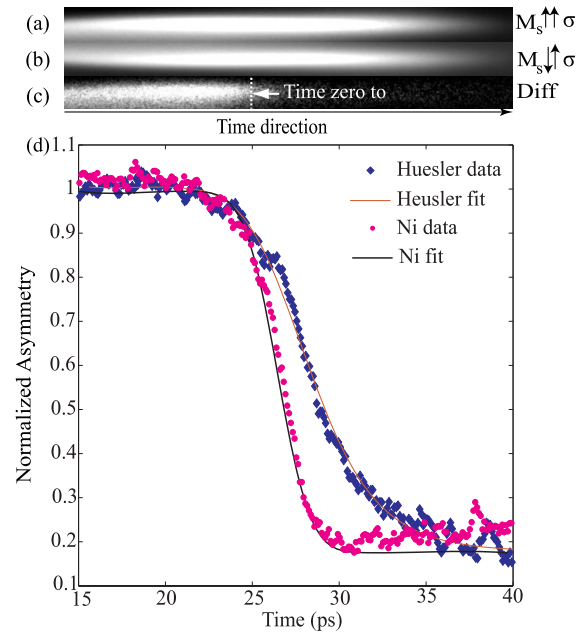


Figure 3. (a) and (b) XMCD transmission streaks at the Mn L_3 edge 639.4 eV, with magnetization orientation anti-parallel and parallel to the polarization of incident x-ray pulses. A difference streak is shown in (c). (d) Normalized Ni and Co_2MnSi asymmetry signals and fits. Data collected at a laser power of ~ 250 mW.

and Heusler data in temporal proximity, in order to minimize systematic error. Ni demagnetization curves were measured immediately before and after the Co_2MnSi measurement, while keeping the laser and streak camera setup unchanged. The experimental Ni demagnetization was constant within given error bars. The Heusler mean lifetime constant was determined by assuming that the demagnetization follows a simple first order rate equation and fitting the Co_2MnSi cross section with a convolution of an exponential and a Gaussian (detector resolution) function. A simple exponential decay indicates a process that is governed by a universal time constant and modulated by the occupation of a single reservoir, e.g., the number of available empty minority states. Exponential decay functions have been frequently used as a fit function for the demagnetization of simple ferromagnets, however more complicated demagnetization profile have been observed in some systems. As demonstrated by the quality of the fit in figure 3(d), an exponential decay models the demagnetization of Co_2MnSi well. These fits produced a $2\sigma = 2.2 \pm 0.1$ ps for the detector resolution and were used to determine the Heusler demagnetization mean lifetime, $\tau = 3.5 \pm 0.5$ ps. The Ni and Co_2MnSi demagnetization cross section asymmetries and fits are shown side by side in figure 3(d) in order to demonstrate the remarkable differences in the demagnetization rates of these materials.

3.1. Laser aging of Co_2MnSi

Throughout the duration of the experiment, the Co_2MnSi sample was exposed to laser pulses with extremely high photon densities for up to ten consecutive hours at a time and cyclically

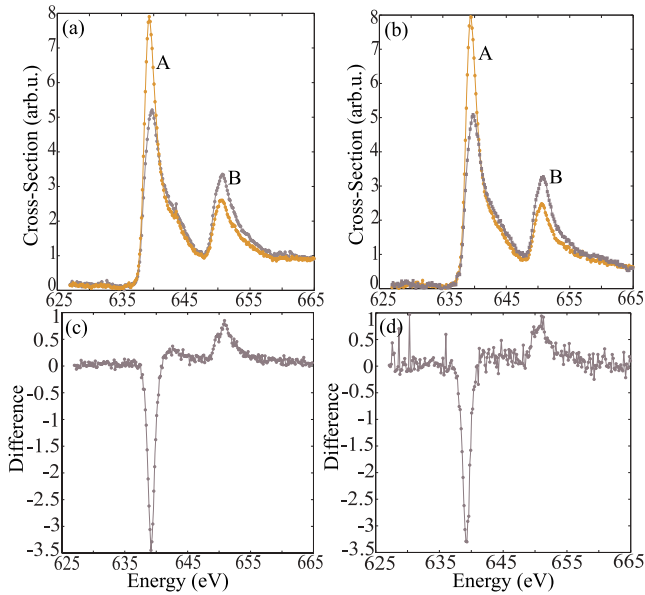


Figure 4. XMCD spectra collected at the Mn L_3 and L_2 edges before laser exposure shown in panel (a) and after exposure (b). The data in orange (A) was collected with M_s orientation parallel to the x-ray polarization and that in purple (B) taken for M_s anti-parallel to the x-ray polarization. The lower figure panels (c) and (d) show the difference signal obtained by subtracting the I^- (A) and I^+ (B) spectra, respectively.

heated to temperatures close to T_c (~ 985 K). Although the duty cycle was very short (~ 60 fs pulse duration at 5 kHz) there remained the possibility that changes were induced in the magnetic properties of the material. The aging properties of Co_2MnSi were explored by heating a single area of the sample for 6 h at laser powers as high as ~ 260 mW and by taking XMCD spectra at the Mn $L_{2,3}$ edges before and after laser exposure, see figure 4. The mean demagnetization lifetime was collected throughout the heating experiment, showing little change and remaining constant at $\tau = 3.5 \pm 0.5$ ps for six consecutive hours of laser exposure. The cross section spectra shown in the top two panels of figure 4 were collected in transmission at room temperature (RT) and were further used to extract the corresponding difference spectra shown in the bottom panels of figure 4. Very little discrepancy is seen in the collected XMCD and difference spectra, implying that the magnetic properties of the sample were unaffected by laser heating. It is clear from these results that the mean lifetime and the magnetic properties of our samples remained unchanged even after being cyclically cooled and heated for six consecutive hours. This data set also illustrates the timing stability of our setup and the reproducibility of the demagnetization time in repeated measurements.

3.2. Power dependence of the Co_2MnSi demagnetization time constant

Varied incident photon densities were used to determine if the imperfect ordering in the material and the consequent low lying empty minority states near the Fermi level had any effect on the demagnetization dynamics. The presence of a

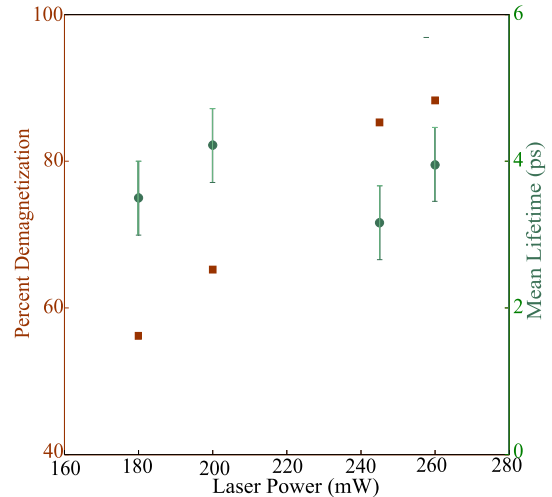


Figure 5. Left axis: per cent demagnetization with respect to asymmetry signal before t_0 , plotted against the incident laser power (squares). Right axis: mean demagnetization lifetime, τ , as a function of laser power (circles).

small number of empty minority states may be evidenced by a fast demagnetization process available at low laser powers in a regime below saturation. To study such an effect, the mean demagnetization life time, τ , of Co_2MnSi was extracted from data accumulated at laser powers of 180–260 mW, corresponding to demagnetization in the range of 55–87%. All measurements were collected consecutively and from the same irradiated spot. The per cent demagnetization values, i.e. per cent of asymmetry signal loss after laser heating at t_0 , are presented as a function of incident laser power (squares) in figure 5. The loss of spontaneous magnetization, M_s , appears to scale approximately linearly with power which verifies that the peak temperature reached by the sample increases monotonically with laser power. The resulting Co_2MnSi mean demagnetization lifetime constants, shown in figure 5 (circles), remained independent of laser power, at an average of 3.5 ± 0.5 ps. This result implies that even at our lowest incident powers the demagnetization is still in a regime where it is strongly bottlenecked.

4. Discussion

Our observation of a demagnetization time above 1 ps remarkably deviates from numerous time-resolved measurements of a wide range of systems, in particular in Ni [1, 4–6, 26], as well as in Co [3, 27] and in Gd [28]. At the used experimental laser power less than 0.1 valence electrons are excited above E_F (per formula unit), far less than the imbalance in occupation of majority and minority states, i.e. $\sim 5 \mu_B/\text{f.u.}$ for a perfectly ordered systems at 0 K. The observed substantial demagnetization therefore relies on the generation of additional hot carriers by electron–electron scattering and their subsequent scattering into minority states. A half-metallic character and minority state band gap of Co_2MnSi at the Fermi level could inhibit the spin-flip scattering processes, in particular in the regime of large demagnetizations ($> 50\%$), explaining our observation.

The consequence is a remarkably slower demagnetization of the studied half-metallic Heusler system in comparison to the conventional ferromagnet Ni [7, 8]. Because of the lack of minority states a half-metal has to demagnetize via an alternate process: either through a loss of long range order via the generation of magnons and transfer of angular momentum by the magneto-crystalline anisotropy [29] while the local atomic magnetization stays initially intact, or by a collapse of the minority states gap followed or accompanied by the spin-flip process that redistributes the minority and majority occupation. Either of these alternate processes appears to occur at a distinctly slower speed.

In the limit of large laser excitations we do not observe the fast, sub-picosecond demagnetization of Co₂MnSi seen by Müller *et al* [10] using the magneto-optical Kerr effect. However, we cannot rule out an initial, fast demagnetization component below our temporal resolution that is followed by a slower demagnetization leading to the almost total demagnetization of the film. The differences in the measured demagnetization times of the samples may be attributed to lower excitation power densities used by Müller *et al* [10], i.e. 1 μ J/pulse versus 50 μ J/pulse used in this work, and a lesser degree of demagnetization achieved⁸. While the Heusler layers were prepared by using similar techniques in both studies, some important differences should be noted: in this study an optimized target was used leading to nearly perfect stoichiometry of the films. The Heusler thickness was chosen to match the penetration depth of the IR pump beam and the demagnetization of the film was measured in transmission, thus probing the entire film. The demagnetization times observed in this work fall in between the ultrafast demagnetization times measured in Ni and the three orders of magnitude slower demagnetization times of established half-metallic systems. Although Co₂MnSi is likely not a perfect half-metal characterized by a spin polarization of close to 100%, in the limit of large demagnetization, we have shown that a residual half-metallic character is maintained. This intermediate position between metals and half-metals fits well into the scheme suggested by Müller *et al*, which connects polarization and demagnetization times across a variety of materials.

5. Conclusions

Our results show evidence for a slow demagnetization process in the Heusler alloy Co₂MnSi as compared to a normal itinerant ferromagnet, Ni. Unlike in ferromagnetic Ni that typically demagnetizes on sub-picosecond timescales, the demagnetization lifetime of Co₂MnSi was measured to be $\sim 3.5 \pm 0.5$ ps. This observation is attributed to a minority states band gap in the DOS of the Co₂MnSi, which inhibits the ultrafast Elliot–Yafet type mechanism that is available to conventional ferromagnetic metals. Future work aimed at determining the demagnetization mechanism can include, for instance, time-dependent spin polarized photoemission measurements to verify a change in the density of states. Sub-picosecond measurements capable of separating the spin and orbital moment can also help in understanding the role the spin–orbit interaction plays on ultrafast timescales.

⁸ Private communication.

Acknowledgments

This work was supported by the director, Office of Science, Office of Basic Energy Sciences, of the US Department of Energy under contract No. DE-AC02-05CH11231 a Laboratory Directed Research and Development Program. This research also constitutes part of a PhD dissertation submitted by Y P Opachich to the University of California at Davis with support from a GANN fellowship from the Department of Education.

References

- [1] Beaurepaire E, Merle J C, Daunois A and Bigot J Y 1996 *Phys. Rev. Lett.* **76** 4250–3
- [2] Dürr H A 2009 *Nucl. Instrum. Methods Phys. Res. A* **601** 132–8
- [3] Güdde J, Conrad U, Jahnke V, Hohlfeld J and Matthias E 1999 *Phys. Rev. B* **59** R6608–11
- [4] Hohlfeld J, Matthias E, Knorren R and Bennemann K H 1997 *Phys. Rev. Lett.* **78** 4861–4
- [5] Rhie H-S, Dürr H A and Eberhardt W 2003 *Phys. Rev. Lett.* **90** 247201
- [6] Scholl A, Baumgarten L, Jacquemin R and Eberhardt W 1997 *Phys. Rev. Lett.* **79** 5146–9
- [7] Koopmans B, Kicken H H J E, Van Kampen M and de Jonge W J M 2005 *J. Magn. Magn. Mater.* **286** 271–5
- [8] Koopmans B, Ruigrok J J M, Longa F D and de Jonge W J M 2005 *Phys. Rev. Lett.* **95** 267207
- [9] Averitt R D and Taylor A J 2002 *J. Phys.: Condens. Matter* **14** R1357
- [10] Müller G M *et al* 2009 *Nat. Mater.* **8** 56
- [11] Kise T, Ogasawara T, Ashida M, Tomioka Y, Tokura Y and Kuwata-Gunokami M 2000 *Phys. Rev. Lett.* **85** 1986
- [12] Ogasawara T, Matsubara M, Tomioka Y, Kuwata-Gonokami M, Okamoto H and Tokura Y 2003 *Phys. Rev. B* **68** 180407
- [13] Ogasawara T, Ohgushi K, Tomioka Y, Takahashi K S, Okamoto H, Kawasaki M and Tokura Y 2005 *Phys. Rev. Lett.* **94** 087202
- [14] Brown P J, Neumann K U, Webster P J and Ziebeck K R A 2000 *J. Phys.: Condens. Matter* **12** 1827
- [15] Galanakis I, Mavropoulos P and Dederichs P H 2006 *J. Phys. D: Appl. Phys.* **39** 765–75
- [16] Mathon J and Umerski A 2001 *Physics of Low Dimensional Systems* ed J Moran-Lopez (New York: Kluwer Academic/Plenum) p 363
- [17] Kämmerer S, Thomas A, Hütten A and Reiss G 2004 *Appl. Phys. Lett.* **85** 79–81
- [18] Schmalhorst J *et al* 2007 *Phys. Rev. B* **75** 014403
- [19] Sasaki S 1994 *Nucl. Instrum. Methods Phys. Res. A* **347** 83
- [20] Warwick T, McKinney W, Domning E, Doran A and Padmore H 2006 *Proc. of the 9th Int. Conf. on Synchrotron Radiation Instrumentation (Daegu, Korea) (AIP Conf. Proc.)* vol 879 pp 469–72
- [21] Carra P, Thole B T, Altarelli M and Wang X 1993 *Phys. Rev. Lett.* **70** 694
- [22] Stöhr J 1999 *J. Magn. Magn. Mater.* **200** 470–97
- [23] Bartelt A F, Comin A, Feng J, Nasiatka R, Eimüller T, Ludescher B, Schütz G, Padmore H A, Young A T and Scholl A 2007 *Appl. Phys. Lett.* **90** 162503
- [24] Feng J *et al* 2007 *Appl. Phys. Lett.* **91** 134102
- [25] Feng J *et al* 2005 *Proc. SPIE* **5920** 592009
- [26] Stamm C *et al* 2007 *Nat. Mater.* **6** 740
- [27] Aeschlimann M, Bauer M, Pawlik S, Weber W, Burgermeister R, Oberli D and Siegmann H C 1997 *Phys. Rev. Lett.* **79** 5158
- [28] Lisowski M, Loukakos P A, Melnikov A, Radu I, Ungureanu L, Wolf M and Bovensiepen U 2005 *Phys. Rev. Lett.* **95** 137402
- [29] Hübner W and Bennemann K H 1996 *Phys. Rev. B* **53** 3422